Environmental cholera (*Vibrio cholerae)* dynamics in an estuarine system in southern coastal Ecuador

RH: Dynamics of Vibrio cholerae in southern Ecuador

Sadie J. Ryan*[1,2], Anna M. Stewart Ibarra[3], Eunice Ordóñez[4], Winnie Chu[5], Julia L. Finkelstein[5], Christine A. King[6], Luis E. Escobar[3,7], Christina Lupone[3], Froilan Heras[3], Erica Tauzer[3], Egan Waggoner[3], Tyler G. James[1,2], Washington B. Cárdenas[4], Mark Polhemus[3]

*Corresponding author: sjryan@ufl.edu, (352) 294-7513

1. Department of Geography and Emerging Pathogens Institute. University of Florida, Gainesville, FL, USA.
2. Emerging Pathogens Institute. University of Florida, Gainesville, FL, USA.
3. Center for Global Health and Translational Science, SUNY Upstate Medical University, Syracuse, NY, USA.
4. Laboratorio de Biomedicina, FCV, Escuela Superior Politécnica del Litoral, Guayaquil, Ecuador.
5. Division of Nutritional Sciences, Cornell University, Ithaca NY, USA
6. Department of Microbiology and Immunology, SUNY Upstate Medical University, Syracuse, NY, USA.
7. Department of Fisheries, Wildlife, and Conservation Biology, University of Minnesota, Saint Paul, MN, USA.

Keywords: Cholera, Ecuador, *Vibrio cholerae*, strains O1 and O139, *Vibrio*, temperature, spatial

Word count: 3616

Acknowledgments

We would like to thank the citizens and authorities of Machala, Ecuador, for their continued support of our research infectious diseases epidemiology and monitoring. This project was supported under a grant from DOD-GEIS P0435_14_UN. The authors have no conflict of interests.

Abstract

Cholera emergence is strongly linked to local environmental and ecological context. The 1991-2004 pandemic emerged in Perú and spread north into Ecuador's El Oro province, making this a key site for potential re-emergence. Machala, El Oro, is a port city of 250,000, near the Peruvian border. Many livelihoods depend on the estuarine system, from fishing for subsistence and trade, to domestic water use. In 2014, we conducted biweekly sampling for 10 months in five estuarine locations, across a gradient of human use, and ranging from inland to ocean. We measured water-specific environmental variables implicated in cholera growth and persistence: pH, temperature, salinity, and algal concentration, and evaluated samples in 5 months for pathogenic and non-pathogenic *Vibrio cholerae*, by polymerase chain reaction (PCR). We found environmental persistence of pandemic strains O1 and O139, but no evidence for toxigenic strains. Cholera presence was coupled to algal and salinity concentration, and sites exhibited considerable seasonal and spatial heterogeneity. This study indicates that environmental conditions in Machala are optimal for cholera re-emergence, with risk peaking during September, and higher risk near urban periphery low-income communities. This highlights a need for surveillance of this coupled cholera– estuarine system to anticipate potential future cholera outbreaks.

Introduction

Cholera remains a severe global threat to public health and development efforts (WHO 2013). According to the World Health Organization, the burden of cholera is at least 100 times greater than current estimates (Zuckerman et al. 2007; WHO 2013), with 120,000 deaths and 3-5 million cases each year worldwide. Previous studies suggest that outbreaks of cholera can be explained by oceanographic variables (e.g., sea surface temperature, pH, salinity) and phytoplankton blooms, indicating the potential to predict disease outbreaks (Jutla et al. 2010; Jutla et al. 2013). A recent analysis of global cholera pandemics indicates that cholera outbreaks originate in coastal regions, often during flood events, before spreading inland (Jutla et al. 2010). Our own previous work suggests that both current and future coastal hotspots of cholera transmission are far larger than current surveillance efforts can capture, with considerably higher potential exposure than previously estimated (Escobar et al. 2015). Estuarine systems are a natural intersection of coastal oceanographic conditions and human use; as productive systems for fisheries, port locations for transport, and rich riparian soils, they are a highly exposed interface for humans. Particularly because coastal estuarine systems often represent subsistence-level dependence on the interface, in terms of artisanal fisheries, a higher likelihood of direct water use, and simply greater physical exposure by proximity, it is also the most vulnerable of populations that are most likely to be exposed to pathogens and the most flooding prone areas in the world (Nicholls 1995; Dixon et al. 2006; De Sherbinin et al. 2007; Hanson et al. 2011; Hallegatte et al. 2013; Cai et al. 2014).

The causative agent of human cholera, *Vibrio cholerae*, is thought to originate from estuarine waters, based on phylogenetic information and its physiological requirements for growth and persistence (Colwell and Huq 1994; Colwell 2004). *Vibrio cholerae* is endemic in

the Bay of Bengal (Bangladesh and India) and along coastal areas in Latin America (Lipp et al. 2002; Mutreja et al. 2011), and it persists environmentally in riverine, estuarine, and coastal waters around the world (Lipp et al. 2002), Cholera epidemics have been found to follow coastlines (Colwell 1996), and *V. cholerae* can be transmitted to humans via a wide range of marine organisms, including zooplankton, aquatic plants, shellfish, and fish (Vezzulli et al. 2010).

Ecuador is a critical location to understand cholera and other climate and water-sensitive diseases due to its (1) high potential for cholera outbreaks and the high incidence of other climate-sensitive infectious diseases (e.g., leptospirosis, dengue), and (2) the strong influence of oceanographic conditions on local climate and flooding during El Niño events (Rossel et al. 1996; Rossel and Cadier 2009; Hanson et al. 2011; Hallegatte et al. 2013; Cai et al. 2014). Indeed, in January 1991, cholera re-emerged in Latin America after more than a century without cases (Lacey 1995). In Ecuador, the 1991 cholera epidemic emerged in the south of the country from a small fishing village in El Oro Province, and it is suspected that a fisherman introduced the index case was traveling north from Perú (Dixon et al. 2006). From 1991 to 2004 over 90,000 cases of cholera were reported in Ecuador, with most cases from coastal provinces. El Oro and Guayas provinces, located in southern coastal Ecuador, encompassed one of two disease epicenters in the country. Recent studies suggest there is a high risk of a second epidemic in Ecuador due to the presence of important risk factors including the growth of vulnerable urban populations, decreased investment in cholera surveillance and prevention programs, increased flood risk associated with climate change, and a street food culture that includes eating raw shellfish (ceviche) (Malavade et al. 2011). In addition, Guayaquil (Guayas Province), the largest city in Ecuador, has been identified as the third most vulnerable city in the world to future flood

95 risk (Hallegatte et al. 2013). Furthermore, it has been found that in populations with a high
96 prevalence of blood group O, such as in Latin America, illness from cholera is more severe, and
97 the requirements for rehydration and hospitalization of infected individuals are considerably
98 higher (Swerdlow et al. 1994; Nelson et al. 2009). Given these conditions, there is compelling
99 evidence that people in southern coast of Ecuador are a high-risk population and there is a
100 critical need for active cholera surveillance in this region.

101 To address this, we evaluated local variability in the presence of cholera in the estuarine
102 environment surrounding the city of Machala, El Oro province, a site identified as a current and
103 future coastal cholera hotspot (Escobar et al. 2015). We selected five sampling sites associated
104 with estuarine water access in Machala, Ecuador, representing a range of economic and human
105 activity conditions, in addition to different proximity to the ocean. Using water sampling
106 methodology, coupled with laboratory identification of *Vibrio cholerae* bacteria, we assessed the
107 local environmental and pathogenic conditions over a period of ten months. Strengthening
108 climate and water-sensitive infectious disease surveillance systems (WHO 2003; Zuckerman et
109 al. 2007) and further understanding of the role of environmental factors in disease outbreak and
110 transmission over time and space (Sedas 2007; Akanda et al. 2013) are urgently needed to target
111 cholera and other climate and water sensitive diseases.

112

113 **Methodology**

114 **Study Site**

115 Machala is a port city of approximately 250,000 inhabitants, with major economic activities
116 stemming from agriculture (bananas), aquaculture (shrimp farming), and fishing/shellfish
117 collection, both small-scale and semi-industrial scale. Five sampling sites were established

within the Machala estuarine system (Figure 1), selected for maximum heterogeneity, to include highly built urban areas, ports, mangrove, and coastal sampling areas. The five sites were: Isla Jambelí, Boca del Macho, Puerto Bolívar Boca, Puerto Bolívar Adentro, and Héroes de Jambelí. Isla Jambelí site is on the outer edge of the coastal draining estuary, and the entrance to Jambelí is interspersed with mangroves and shrimp farms. Boca del Macho is the open edge of the inner estuary, in open water on shallow sand, with mangroves. Puerto Bolívar Boca is near the mouth of the open harbor, characterized by heavy boat traffic, commercial fishing, and residences lining the waterway, with mangroves and shrimp farming on the far side of the waterway. Puerto Bolívar Adentro is further into the city, along the estuary, characterized by residential low-income housing, with shrimp farms and mangroves across the Héroes waterway. Heroes de Jambelí is the most inland site, characterized by low income and poor quality housing built along mangroves at the edge of the city; outflow from the houses is visible directly into the water (Figure 1). The port city of Machala is an important sentinel surveillance site, due to its location along the Pan American highway, approximately 80km north of the Peruvian border, facilitating significant movement of people and potential pathogens by land and sea.

Water sampling

At each of the five study sites (Figure 1), water sampling was conducted at high tide, twice monthly along a transect with 3 sub-sites spaced 250 m apart, and 3 replicates per subsite. Three 1L surface water samples per subsite were collected in sterile polypropylene bottles, and placed in coolers with ice for transport for the laboratory. For environmental sampling, using a YSI water probe* (600 XLM V2 Sonde), we recorded Surface Temperature (ºC), Conductivity, pH,

Salinity, and Optic-T BGA PE (Phycoerythrin) [blue-green algae] (cells/ml, which we converted to cells/µl for ease of visualization) at each end of the transect.

Laboratory analyses

Water samples were transferred to the laboratory in coolers for *Vibrio cholerae* testing and were processed within 24 hours of collection. For laboratory analysis, a 1L water sample was filtered through a Whatman membrane No. 1 and 0.22 µm membrane (Millipore) by vacuum. Then, 10mL of Phosphate Buffered Saline (PBS) (pH 7.4) was pipetted onto the retained contents on the membrane and gently washed by pipette 15x. The PBS was left on the membrane to incubate at room temperature for 15 minutes prior to collection in 50mL conical tube.

DNA isolation and PCR

Genomic DNA was extracted from bacterial pellet of the previous step with a QIAamp DNA mini kit (Qiagen), following manufacture instructions. Diagnosis of cholera serogroups and the detection of toxigenic genes were performed each by duplex PCR. Table 1 describes primers sets used to amplify the *rfb* region of O1 and O139 serogroups and the toxin subunit A (ctxA) and toxin coregulated pilus (tcpA) genes. For both duplex PCRs, master mix was as follows: 0.05 U/ul of JumpStart REDTaq DNA Polymerase (Sigma), 1X buffer, 0.2 mM dNTPs, 0.2 mM of each primer set, 1 µl of template and ultrapure water to a final volume of 25 µl. The amplification program for diagnosis of serogroups was adapted from Hoshino et al.(Hoshino et al. 1998), using the following conditions: 5 minutes at 94°C, 35 cycles of 94°C for 1 minute, 55°C for 1 minute and 72°C for 1 minute and final extension of 72°C for 7 minutes. Positive samples for either or both serogroups were subjected to toxigenic genes duplex PCR. The

amplification program was according to conditions described in Kumar et al.(Kumar et al. 2010): 3 minutes at 94°C, 30 cycles of 94°C for 30 seconds, 59°C for 30 seconds and 72°C for 1.2 minutes, and final extension of 72°C for 10 minutes. PCR products were resolved in a 2% agarose gel and sequenced to verify gene amplification.

Statistical analyses

As the data were not normally distributed, we conducted non-parametric tests throughout. We characterized the sampling sites for each environmental variable: Temperature, pH, Salinity, and BGA, conducting Kruskal-Wallis rank sum tests on site means, and on monthly means. We then examined whether *V. cholerae* prevalence at sites, and strain (i.e., O1, O139) prevalence separately, was associated with environmental variables using a series of non-parametric Kendall's tau correlations.

Results

Environmental characteristics

The probe recorded a range of 9-104 readings at each sub-site biweekly for 10 months. We pooled all readings by month for analyses. Our sample sites differed significantly in environmental characteristics (Figure 2), as shown by a series of Kruskal-Wallis rank sum tests (Temperature: χ^2= 206.19, df = 4, $p < 0.0001$; Salinity: χ^2= 2257.5, df = 4, $p < 0.0001$; pH: χ^2= 1347.3, df = 4, $p < 0.0001$; BGA χ^2= 1824.8, df = 4, $p < 0.0001$). We found that Héroes de Jambelí, the most inland site, had the highest BGA, and that Isla de Jambelí, the most coastal site, had the highest salinity; while there were statistical differences between all sites in all the environmental variables, there were no clear outliers in the other variables. Our sample sites

exhibited significant change in environmental characteristics across months (Figure 3), as shown by a series of Kruskal-Wallis rank sum tests (Table 2). Temperature was lowest in August for all sites – likely reflecting pacific upwelling, which cools the water, regardless of air temperature. Salinity at the most inland site, Héroes de Jambelí, was consistently lowest, and showed the smallest change across months, while the other sites had a decrease in salinity in May, then a rise from July-December. Isla de Jambelí had the highest salinity, reflecting its location on the most coastal site. BGA was highest at the most inland site, Héroes de Jambelí, peaking in May, lagging temperature by a month. BGA shows the least temporal or spatial clustered pattern and has no obvious seasonality across the year. Heroes de Jambeli, however, registered the highest BGA values during the study (~25,000). pH appears to peak in December-January across all sites, with a decrease in July-August; the coastal and inland sites showed low pH values across seasons, while Boca del Macho registered consistently high pH values across months.

Laboratory analyses

Of a total of 405 individual water samples, collected between May – September, 382 were diagnosed by PCR. We found 139 (36.4%) samples positive for *V. cholerae*, and 243 (64%) negative. We found both O1 and O139 serogroups of *V. cholerae* present in the estuarine system studied in Machala, Ecuador. Serogroup O139 was predominant; 118 (83.5%) samples were O139, and 51 (35.3%) were O1 (30 samples contained both). We were able to detect *V. cholerae* during each of the 5 months of sampling, nevertheless we found that prevalence decreased drastically in July (Figure 4). By sequencing the samples, we confirmed that the PCR protocol applied was proper for detection of *V. cholerae* serogroups O1 and O139 strains.

Vibrio cholerae characteristics

We pooled water samples within sites, to derive monthly *V. cholerae* prevalences across and within sites (prevalence = positive/total samples tested). Overall monthly prevalence of *V. cholerae* ranged from 0.3 (n=68) in July to 0.58 (n=45) in September, with site prevalence ranging 0-1, with a mean monthly site prevalence of 0.35 (Figure 4A). Individual strain prevalence was generally higher for O139 than O1, but we see that Puerto Bolívar Adentro and Héroes de Jambelí were *V. cholerae* positive in every month and also had higher prevalences than the other sites (Figure 4B and 4C). We found that the prevalence of *V. cholerae*, and O139 and O1 strains separately, were significantly associated with higher BGA (blue-green algae densities), and that prevalence of *V. cholerae* the O1 strain were significantly associated with lower salinity. We found no significant association between prevalence and temperature or pH (Table 3).

Discussion and Recommendations

We found evidence of an environmental reservoir of *V. cholerae* in the estuarine waters of Machala, Ecuador, in 2014. We confirmed the presence of *V. cholerae*, including pandemic strains O1 and O139. We cannot rule out ongoing toxigenic presence, but we did not detect it in our samples.

Our sites exhibited considerable seasonal and spatial heterogeneity in environmental variables and *V. cholerae* prevalence, with clear peaks (and troughs) during specific months. For example, we found peak *V. cholerae* prevalence in September, with highest values in two sites: – Héroes de Jambelí and Puerto Bolívar Adentro (Figure 1), these sites are characterized by low income housing on the edge of the city, while being inland sites, facing mangroves and shrimp

farms, and were found to have *V. cholerae* present in every month sampled. The lowest *V. cholerae* prevalence was found in July, in which only the two most inland sites had *V. cholerae* detection. Water temperature had the clearest temporal pattern, falling rapidly through July, likely corresponding to Pacific upwelling, cooling the waters, and increasing nutrients in the system (Strutton et al. 2001). We found that there was lowest salinity in the most inland site, Héroes de Jambelí, and a higher concentration of BGA than in other sites. This is in contrast to Isla Jambelí, a small island community furthest from the mainland and closest to the ocean, with high salinity due to its coastal location; however, it did not have lower BGA than other sites.

We found that the timing of *V. cholerae* was coupled to the environmental variables we measured. For example, water temperature, BGA, and pH decreased in most sites through July/August, so did the overall prevalence of *V. cholerae*, but we only demonstrated significant associations between prevalence and site and month specific levels of salinity and BGA. Average ocean salinity is around 35 ppt, while freshwater rivers average around 0.5 ppt; clearly in this estuarine system, we see a mixed or brackish system, ranging from the lower average of around 15 ppt at our most inland site, to a high approaching 34 ppt at our coastal site. We detected *V. cholereae* at a range of salinities, finding a negative correlation with increasing salinity, suggesting that the lower salinity may provide a more suitable environment for the growth of *V. cholereae*, but that even the higher salinity approaching ocean concentrations do not prevent that growth. This finding is consistent with previous work demonstrating the suitability of coastal oceans for *V. cholereae*(Strutton et al. 2001), but reveals a finer scale relationship with salinity as we move inland in an estuarine system, up the gradient to fresh water.

BGA (blue-green algae; a.k.a. cyanobacteria) are photosynthetic prokaryotes that can be found in freshwater, marine, and terrestrial environments (Stanier and Bazine 1977). The

255 photosynthetic pigments of cyanobacteria include chlorophyll-*a* and the phycobiliprotein
256 phycoerythrin. Here we use BGA values to characterize water features and because BGA has
257 been associated with *V. cholereae* persistence (Epstein 1993). However, BGA itself also poses a
258 significant threat to humans through its production of cyanotoxins. BGA toxins include
259 neurotoxins, hepatotoxins, cytotoxins, irritants and gastrointestinal toxins (Codd et al. 2005).
260 Among these chemicals, microsystin, is a known liver carcinogen (Hunter 1998), and has been
261 detected in marine ecosystems (Miller et al. 2010). Exposure to these via skin contact, inhalation,
262 or ingestion, can result in a range of effects, from skin irritation and conjunctivitis, to kidney
263 damage and respiratory arrest (Codd et al. 1999). The World Health Organization (WHO)
264 recognizes BGA blooms as an emerging public health risk, and recommends the development of
265 early warning systems to detect scums (World Health Organization 1999; Falconer 2001;
266 Manganelli et al. 2012). We argue that BGA related diseases should be included in differential
267 diagnosis in Héroes de Jambelí, particularly during May, when a BGA increase was evident in
268 this study.

269 Temperature increase, coupled with high nutrient load, low flow, and thermal
270 stratification, generally results in increased growth rates of cyanobacteria, and its dominance in
271 the phytoplankton community (Davis et al. 2009; Elliott 2010; Huber et al. 2012). This could
272 explain the high BGA values early in the year (Figure 3). In addition, warm temperatures
273 promote increases in the number of days where BGA biomass exceeds thresholds established by
274 WHO (Davis et al. 2009; Elliott 2012). High temperature influences water column stability and
275 mixing depth, producing favorable conditions for BGA blooms (Robarts and Zohary 1987; Stal
276 et al. 2003). This association of temperature increase with BGA blooms is consistent across
277 coastal, estuarine, and inland waters (Paerl 1988). Thus, long term monitoring to measure BGA

biomass should be considered at least in Heroes de Jambeli and Puerto Bolivar -the sites report the highest BGA values (Figure 2), particularly considering that a rise in water temperature is associated with BGA emergence (Wasmund 1997; Kanoshina et al. 2003; Suikkanen et al. 2007), increasing the risk of BGA diseases with imminent future climate warming.

In Ecuador, seawater eutrophication is a public health problem (World Health Organization 1999).In fact, several species of BGA have been identified in aquatic environments in Ecuador (Gunkel and Casallas 2002; Nedbalová and Sklenár 2008; Ramírez-Luna et al. 2008). Unfortunately, while there is an increasing recognition of the negative health effects of BGA blooms, monitoring in coastal marine waters is rare, and efforts are strongly biased to freshwater systems (Nedbalová and Sklenár 2008), making our exploration in estuarine areas a crucial update to the status of BGA in the country. This study was conducted in an average climate year, providing a preliminary framework for monitoring coupled *V. cholerae* – estuarine dynamics for potential emergence of cholera outbreaks in the region. This is particularly useful baseline information for anticipating El Niño years, extreme climate events associated with warming temperatures of surface ocean water and increased rainfall and flooding events. Climate change projections indicate that the frequency of extreme El Niño events will increase in the future, (Cai et al. 2014) increasing the risk of water-borne diseases endemic in the region, such as cholera, typhoid, and leptospirosis, and provides valuable information to add *V. cholerae* in the public health agenda to consider infectious diseases beyond the already important vector-borne diseases, such as dengue fever, chikungunya, zika, and malaria.

Indeed, by May 2016, two years after the initiation of this study, the first case of cholera was reported in Machala, after approximately 12 years with no case reports in Ecuador (2016). An immuno-compromised individual was confirmed positive for *V. cholerae* serotype O1 non-

toxigenic, by the National Public Health Research Institute of the Ministry of Health. Our team diagnosed the patient using the same PCR assay described here. Although the source of the infection was not confirmed, this case report suggests a worrisome link to the results of our epidemiological survey, and merits further examination.

This study highlights the urgency for active epidemiological surveys and the need for public health interventions to reduce the risk of water-borne pathogens in vulnerable populations from a holistic social-ecological perspective. The community Héroes de Jambelí is a low-income peri-urban settlement with less than 50 families, established informally in 2002. The community continues to lack adequate access to piped water, sewerage, and garbage collection due to their status as an illegal settlement. Simple bamboo homes have built over the mangrove system, with direct discharge of wastewater into the estuary. At the same time, this community's livelihood depends on artisanal fisheries (e.g., crabs, mollusks) from these same estuaries. This vulnerable coupled human-natural system results in high risk of emerging epidemics from water-borne pathogens.

The results of this study, coupled with ongoing and previously published remote sensing and GIS assessments, will allow us to identify geographic areas for future *V. cholerae* surveillance across coastal Ecuador. In the future, we anticipate sampling additional sites where we have identified geographic algal bloom hotspots, but which do not have historic reports of cholera emergence – to serve as control sites for analyses, and to provide background levels of *Vibrio* and other pathogens. This information will inform the development of predictive maps and population attributable fractions to help translate surveillance and modeling data into numbers that can inform policy development, identification of communities at increased risk of cholera, and preventive interventions. Other future projects will include: continued development

of a training program in infectious disease surveillance, development of a web-based GIS platform to integrate data sources and examine the role of environmental factors in *V. cholerae* transmission over time and space, and development of an early warning system for climate-sensitive diseases.

References

Akanda AS, Jutla AS, Gute DM, Sack RB, Alam M, Huq A, Colwell RR, Islam S (2013) Population Vulnerability to Biannual Cholera Outbreaks and Associated Macro-Scale Drivers in the Bengal Delta.

Cai W, Borlace S, Lengaigne M, Van Rensch P, Collins M, Vecchi G, Timmermann A, Santoso A, McPhaden MJ, Wu L (2014) Increasing frequency of extreme El Niño events due to greenhouse warming. Nat Clim Change 4:111–116.

Codd GA, Bell SG, Kaya K, Ward CJ, Beattie KA, Metcalf JS (1999) Cyanobacterial toxins, exposure routes and human health. Eur J Phycol 34:405–415.

Codd GA, Morrison LF, Metcalf JS (2005) Cyanobacterial toxins: risk management for health protection. Toxicol Appl Pharmacol 203:264–272.

Colwell RR (2004) Infectious disease and environment: cholera as a paradigm for waterborne disease. Int Microbiol 7:285–289.

Colwell RR (1996) Global climate and infectious disease: the cholera paradigm. Science 274:2025.

Colwell RR, Huq A (1994) Environmental Reservoir of Vibrio cholerae The Causative Agent of Choleraa. Ann N Y Acad Sci 740:44–54. doi: 10.1111/j.1749-6632.1994.tb19852.x

Davis TW, Berry DL, Boyer GL, Gobler CJ (2009) The effects of temperature and nutrients on the growth and dynamics of toxic and non-toxic strains of Microcystis during cyanobacteria blooms. Harmful Algae 8:715–725.

De Sherbinin A, Schiller A, Pulsipher A (2007) The vulnerability of global cities to climate hazards. Environ Urban 19:39–64.

Dixon TH, Amelung F, Ferretti A, Novali F, Rocca F, Dokka R, Sella G, Kim S-W, Wdowinski S, Whitman D (2006) Space geodesy: Subsidence and flooding in New Orleans. Nature 441:587–588.

Elliott A (2012) Predicting the impact of changing nutrient load and temperature on the phytoplankton of England's largest lake, Windermere. Freshw Biol 57:400–413.

Elliott J (2010) The seasonal sensitivity of cyanobacteria and other phytoplankton to changes in flushing rate and water temperature. Glob Change Biol 16:864–876.

Epstein PR (1993) Algal blooms in the spread and persistence of cholera. Biosystems 31:209–221.

Escobar LE, Ryan SJ, Stewart-Ibarra AM, Finkelstein JL, King CA, Qiao H, Polhemus ME (2015) A global map of suitability for coastal Vibrio cholerae under current and future climate conditions. Acta Trop 149:202–211.

Falconer IR (2001) Toxic cyanobacterial bloom problems in Australian waters: risks and impacts on human health. Phycologia 40:228–233.

Gunkel G, Casallas J (2002) Limnology of an equatorial high mountain lake—Lago San Pablo, Ecuador: the significance of deep diurnal mixing for lake productivity. Limnol-Ecol Manag Inland Waters 32:33–43.

367 Hallegatte S, Green C, Nicholls RJ, Corfee-Morlot J (2013) Future flood losses in major coastal
368 cities. Nat Clim Change 3:802–806.

369 Hanson S, Nicholls R, Ranger N, Hallegatte S, Corfee-Morlot J, Herweijer C, Chateau J (2011)
370 A global ranking of port cities with high exposure to climate extremes. Clim Change
371 104:89–111.

372 Hoshino K, Yamasaki S, Mukhopadhyay AK, Chakraborty S, Basu A, Bhattacharya SK, Nair
373 GB, Shimada T, Takeda Y (1998) Development and evaluation of a multiplex PCR assay
374 for rapid detection of toxigenic Vibrio cholerae O1 and O139. FEMS Immunol Med
375 Microbiol 20:201–207.

376 Huber V, Wagner C, Gerten D, Adrian R (2012) To bloom or not to bloom: contrasting
377 responses of cyanobacteria to recent heat waves explained by critical thresholds of abiotic
378 drivers. Oecologia 169:245–256.

379 Hunter P (1998) Cyanobacterial toxins and human health. J Appl Microbiol 84:35–40.

380 Jutla A, Akanda AS, Huq A, Faruque ASG, Colwell R, Islam S (2013) A water marker
381 monitored by satellites to predict seasonal endemic cholera. Remote Sens Lett 4:822–
382 831.

383 Jutla AS, Akanda AS, Islam S (2010) Tracking Cholera in Coastal Regions Using Satellite
384 Observations1. JAWRA J Am Water Resour Assoc 46:651–662.

385 Kanoshina I, Lips U, Leppänen J-M (2003) The influence of weather conditions (temperature
386 and wind) on cyanobacterial bloom development in the Gulf of Finland (Baltic Sea).
387 Harmful Algae 2:29–41.

388 Kumar P, Peter WA, Thomas S (2010) Rapid detection of virulence-associated genes in
389 environmental strains of Vibrio cholerae by multiplex PCR. Curr Microbiol 60:199–202.

390 Lacey SW (1995) Cholera: calamitous past, ominous future. Clin Infect Dis 20:1409–1419.

391 Lipp EK, Huq A, Colwell RR (2002) Effects of global climate on infectious disease: the cholera
392 model. Clin Microbiol Rev 15:757–770.

393 Malavade SS, Narvaez A, Mitra A, Ochoa T, Naik E, Sharma M, Galwankar S, Breglia MD,
394 Izurieta R (2011) Cholera in Ecuador: Current relevance of past lessons learnt. J Glob
395 Infect Dis 3:189.

396 Manganelli M, Scardala S, Stefanelli M, Palazzo F, Funari E, Vichi S, Buratti FM, Testai E
397 (2012) Emerging health issues of cyanobacterial blooms. Ann DellIstituto Super Sanità
398 48:415–428.

399 Miller MA, Kudela RM, Mekebri A, Crane D, Oates SC, Tinker MT, Staedler M, Miller WA,
400 Toy-Choutka S, Dominik C (2010) Evidence for a novel marine harmful algal bloom:
401 cyanotoxin (microcystin) transfer from land to sea otters. PLoS One 5:e12576.

402 Mutreja A, Kim DW, Thomson NR, Connor TR, Lee JH, Kariuki S, Croucher NJ, Choi SY,
403 Harris SR, Lebens M, others (2011) Evidence for several waves of global transmission in
404 the seventh cholera pandemic. Nature 477:462–465.

405 Nedbalová L, Sklenár P (2008) New records of snow algae from the Andes of Ecuador. Arnaldoa
406 15:17–20.

407 Nelson EJ, Harris JB, Morris JG, Calderwood SB, Camilli A (2009) Cholera transmission: the
408 host, pathogen and bacteriophage dynamic. Nat Rev Microbiol 7:10.1038/nrmicro2204.
409 doi: 10.1038/nrmicro2204

410 Nicholls RJ (1995) Coastal megacities and climate change. GeoJournal 37:369–379.

411 Paerl HW (1988) Nuisance phytoplankton blooms in coastal, estuarine, and inland waters.
412 Limnol Oceanogr 33:823–843.

413 Ramírez-Luna V, Navia AF, Rubio EA (2008) Food habits and feeding ecology of an estuarine
414 fish assemblage of northern Pacific Coast of Ecuador. Pan-Am J Aquat Sci 3:361–372.

415 Robarts RD, Zohary T (1987) Temperature effects on photosynthetic capacity, respiration, and
416 growth rates of bloom□forming cyanobacteria. N Z J Mar Freshw Res 21:391–399.

417 Rossel F, Cadier E (2009) El Niño and prediction of anomalous monthly rainfalls in Ecuador.
418 Hydrol Process 23:3253–3260. doi: 10.1002/hyp.7401

419 Rossel F, Cadier E, Gómez G (1996) Las inundaciones en la zona costera ecuatoriana: causas ---
420 obras de protección existentes y previstas. l'Institut francais d'études Andines (IFE)

421 Sedas VTP (2007) Influence of environmental factors on the presence of Vibrio cholerae in the
422 marine environment: a climate link. J Infect Dev Ctries 1:224–241.

423 Stal LJ, Albertano P, Bergman B, von Bröckel K, Gallon JR, Hayes PK, Sivonen K, Walsby AE
424 (2003) BASIC: Baltic Sea cyanobacteria. An investigation of the structure and dynamics

425 of water blooms of cyanobacteria in the Baltic Sea—responses to a changing
426 environment. Cont Shelf Res 23:1695–1714.

427 Stanier R, Bazine G (1977) Phototrophic prokaryotes: the cyanobacteria. Annu Rev Microbiol
428 31:225–274.

429 Strutton PG, Ryan JP, Chavez FP (2001) Enhanced chlorophyll associated with tropical
430 instability waves in the equatorial Pacific. Geophys Res Lett 28:2005–2008.

431 Suikkanen S, Laamanen M, Huttunen M (2007) Long-term changes in summer phytoplankton
432 communities of the open northern Baltic Sea. Estuar Coast Shelf Sci 71:580–592.

433 Swerdlow DL, Mintz ED, Rodriguez M, Tejada E, Ocampo C, Espejo L, Barrett TJ, Petzelt J,
434 Bean NH, Seminario L (1994) Severe life-threatening cholera associated with blood
435 group 0 in peru: implications for the latin american epidemic. J Infect Dis 170:468–472.

436 Vezzulli L, Pruzzo C, Huq A, Colwell RR (2010) Environmental reservoirs of Vibrio cholerae
437 and their role in cholera. Environ Microbiol Rep 2:27–33.

438 Wasmund N (1997) Occurrence of cyanobacterial blooms in the Baltic Sea in relation to
439 environmental conditions. Int Rev Gesamten Hydrobiol Hydrogr 82:169–184.

440 WHO (2013) Cholera Annual Report. Wkly Epidemiol Rec 321–336.

441 WHO (2003) Cholera Unveiled: Global Task. Force on Cholera Control. World Health
442 Organization Geneva

443 World Health Organization (1999) Toxic Cyanobacteria in Water: A guide to their public health
444 consequences, monitoring and management.

445 Zuckerman JN, Rombo L, Fisch A (2007) The true burden and risk of cholera: implications for
446 prevention and control. Lancet Infect Dis 7:521–530.

447 (2016) Epidemiological Update: Cholera. 27 May, Washington, D.C.: PAHO/WHO; 2016. Pan
448 American Health Organization / World Health Organization., Washington, D.C.

449

450

451

452 **Table 1.** PCR primers set used in this study

Set	Primer	Sequence	Product	Reference
1	O1F2-1	GTT TCA CTG AAC AGA TGG G	192 bp	(Hoshino et al. 1998) Development and evaluation of a multiplex PCR assay for rapid detection of toxigenic *Vibrio cholerae* O1 and O139
	O1R2-2	CGG TCA TCT GTA AGT ACA AC		
2	O139F2	AGC CTC TTT ATT ACG GGT GG	449bp	
	O139R2	GTC AAA CCC GAT CGT AAA GG		
3	tcpA-F	ATG CAA TTA TTA AAA CAG CTT TTT AAG	675bp	(Kumar et al. 2010) Rapid Detection of Virulence-Associated Genes in Environmental Strains of *Vibrio cholerae* by Multiplex PCR
	tcpA-R	TTA GCT GTT ACC AAA TGC AAC AG		
4	ctxA-F	CGG GCA GAT TCT AGA CCT CCT G	564bp	(Singh et al. 2002) Development of a hexaplex PCR assay for rapid detection of virulence and regulatory genes in *Vibrio cholerae* and *Vibrio mimicus*
	ctxA-R	CGA TGA TCT TGG AGC ATT CCC AC		

453

454

455 **Table 2.** Kruskal-Wallis rank sum test results for each site and environmental variable

456 differences by month.

457

Environmental Variable	***Site***	X^2	***DF***	***p-value***
Temperature	Boca de Macho	832.65	9	0.0001
	Héroes de Jambelí	643.85	8	0.0001
	Isla de Jambelí	622.85	9	0.0001
	Puerto Bolívar Adentro	445.99	9	0.0001
	Puerto Bolívar Boca	625.44	9	0.0001
Salinity				
	Boca de Macho	837.16	9	0.0001
	Héroes de Jambelí	230.17	8	0.0001
	Isla de Jambelí	671.41	9	0.0001
	Puerto Bolívar Adentro	464.85	9	0.0001
	Puerto Bolívar Boca	619.21	9	0.0001
pH				
	Boca de Macho	534.3	9	0.0001
	Héroes de Jambelí	431.66	8	0.0001
	Isla de Jambelí	245.91	9	0.0001
	Puerto Bolívar Adentro	378.53	9	0.0001
	Puerto Bolívar Boca	416.76	9	0.0001
BGA				
	Boca de Macho	650.84	9	0.0001
	Héroes de Jambelí	309.2	8	0.0001
	Isla de Jambelí	469.75	9	0.0001
	Puerto Bolívar Adentro	219.78	9	0.0001
	Puerto Bolívar Boca	519.81	9	0.0001

458

459 **Table 3:** Kendall tau tests for correlation between prevalence of cholera, and each strain

460 separately, and environmental variables at sites, pooled monthly.

461

Environmental Variable	**Prevalence**	**Kendall's τ**	**z**	***p*-value**
Temperature	*V. cholerae*	0.08	0.56	0.57
	O1	0.12	0.80	0.42
	O139	0.02	0.12	0.91
Salinity	*V. cholerae*	-0.34	-2.35	**0.02**
	O1	-0.35	-2.29	**0.02**
	O139	-0.28	-1.92	0.06
pH	*V. cholerae*	-0.10	-0.68	0.49
	O1	-0.14	-0.92	0.36
	O139	-0.10	-0.64	0.52
BGA	*V. cholerae*	0.55	3.76	**0.00**
	O1	0.48	3.09	**0.00**
	O139	0.49	3.34	**0.00**

462

463

Figures

Figure 1: Location of sampling sites. **A.** Ecuador (in yellow) in South America, indicating the location of Machala (red point); **B.** Location of Machala on the southern coast of Ecuador (red point); **C.** Location of the five sampling sites: Isla Jambelí, Boca del Macho, Puerto Bolívar Boca, Puerto Bolívar Adentro, and Héroes de Jambeli (red points), in and around Machala (green).

Figure 2: Environmental features in the study area. Water characteristics by site (means and standard errors Temperature (TEMP, °C), Salinity (SAL), pH, and measured total concentration of blue-green algae (BGA, cells/µL).

Figure 3: Environmental features in the study period. Water characteristics by month (means and standard errors) and sites: **A**. Temperature (TEMP, °C), **B.** Salinity (SAL), **C.** measured total concentration of blue-green algae (BGA, cells/µL), and **D.** pH.

Figure 4: *Vibrio cholerae* detection. Monthly site prevalence of **A.** cholera as given by positive PCR test, **B.** O1 strain, **C.** O139 strain.

Figure 1

Figure 2

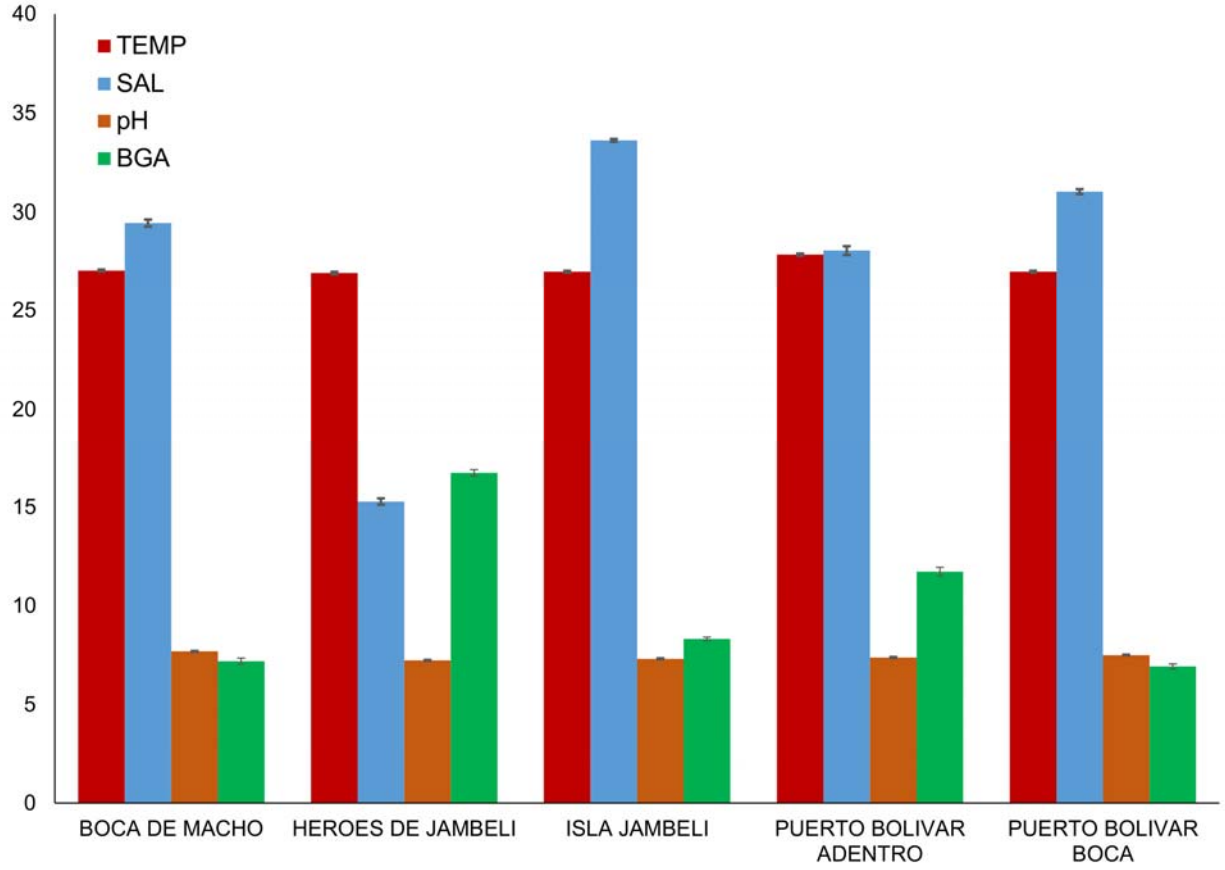

490 **Figure 3**

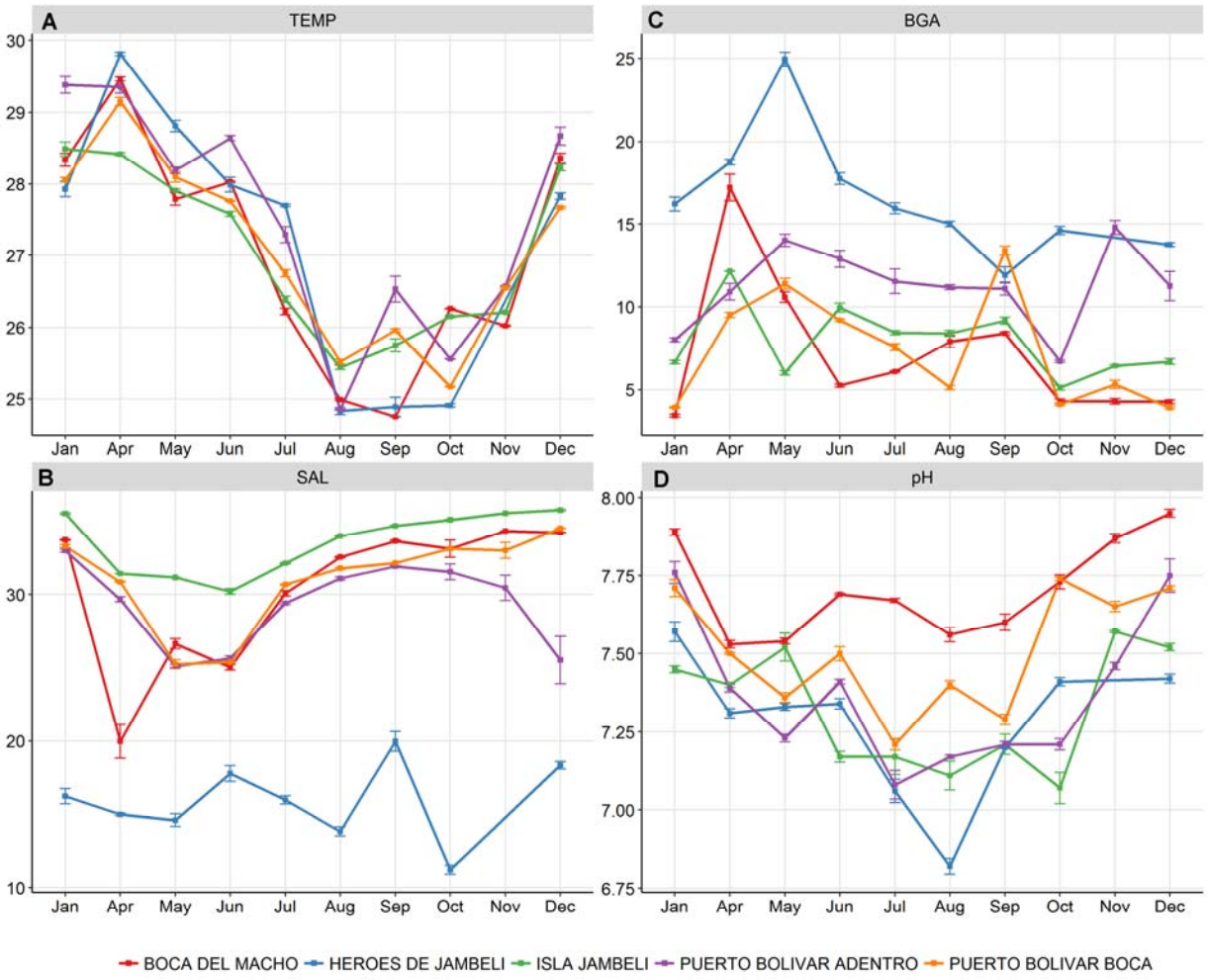

491

492

493 **Figure 4**

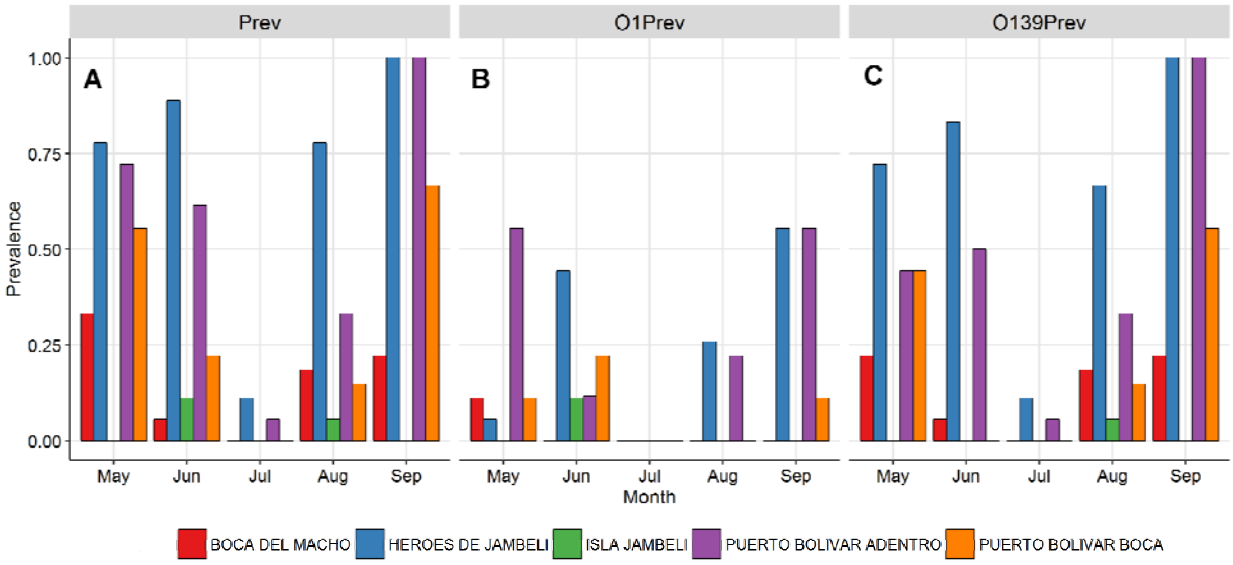

494